frontiers | Frontiers in Earth Science

TYPE Original Research
PUBLISHED 10 January 2023
DOI 10.3389/feart.2022.1120772

OPEN ACCESS

EDITED BY
Naifei Liu,
Xi'an University of Architecture and Technology, China

REVIEWED BY
Jinting Huang,
Xi'an University of Science and Technology, China
Zizhao Zhang,
Xinjiang University, China

*CORRESPONDENCE
Zongyuan Ma,
mzy_gogo@hotmail.com

SPECIALTY SECTION
This article was submitted to Environmental Informatics and Remote Sensing,
a section of the journal Frontiers in Earth Science

RECEIVED 10 December 2022
ACCEPTED 28 December 2022
PUBLISHED 10 January 2023

CITATION
Ma Z, Tang S and Yang Z (2023), Numerical analysis of metro station pit dewatering and its influence.
Front. Earth Sci. 10:1120772.
doi: 10.3389/feart.2022.1120772

Numerical analysis of metro station pit dewatering and its influence

Zongyuan Ma[1,2]*, Shitong Tang[2] and Zhiguo Yang[3]

[1]Guizhou Communications Polytechnic, Guiyang, Guizhou, China, [2]Xi'an University of Technology, Xi'an, Shaanxi, China, [3]China Railway First Survey and Design Institute Group Co., Ltd., Xi'an, Shaanxi, China

The underground water level in Xi'an city is generally shallow, and the excavation of the deep foundation pit mainly needs underground water dewatering. The ground deformation due to the dewatering and its influences should be fully analyzed. The empirical formula estimates the water inflow of the foundation pit, and the process of dewatering and metro station construction is simulated via the finite element method and the theory of soil consolidation according to the field investigation and survey data of the natural geological and hydrological environment. The time of water level falling and recovery, ground settlement, and strata deformation caused by pit dewatering and excavation are predicted. The analysis results of the ground settlement are within reasonable limits and close to the previous metro projects. Finally, the influence of groundwater dewatering on Xi'an Metro Line 14 is discussed. The settlement induced by dewatering for constructing a metro station in the sandy stratum is relatively small, and the loess stratum has the most significant dewatering settlement. The proportion of settlement due to dewatering of the station construction in the loess stratum is nearly 1/3 versus the total land subsidence.

KEYWORDS

metro station, foundation pit, groundwater dewatering, hydraulic discharge prediction, consolidation deformation

1 Introduction

The construction of urban rail traffic is the megacity's critical development target of public transport engineering, and it plays an important role in alleviating urban traffic congestion (Sun et al., 2015). Subway or metro is an emerging urban rail transit mode with the characteristics of being fast and comfortable, less occupation of land resources, large passenger volume, less pollution, and high safety performance. Xi'an metro has entered a new period of vigorous development in recent years, and most of the main lines are built in the downtown area. However, a deep foundation pit must be excavated before the construction of the metro station. The groundwater should be dewatered before the excavation of the foundation pit if the groundwater level exceeds the bottom of the pit. The groundwater extraction should be carried out during the foundation pit construction to reduce the shallow underground water levels (referred to as dewatering) (Shaqour and Hasan, 2008; Pujades et al., 2014; Attard et al., 2016). The seepage of the foundation pit slope and basement will be prevented effectively by dewatering the groundwater level below the bottom of the foundation pit (Attard et al., 2016). Otherwise, the soil strength and the stability of the foundation pit can also be enhanced by decreasing the soil water content. Thus, studying the influence of foundation pit dewatering on the project site and surrounding environment is necessary. Currently, empirical formulas and numerical simulation methods are often used to analyze the influence of the deformation of strata and the land subsidence caused by dewatering on the surrounding buildings and underground pipelines (Zhou et al., 2010; Wang et al., 2013; Pujades et al., 2017; Wang et al., 2022). The deep foundation pit dewatering and ground settlement are efficiently analyzed via the water-soil coupling consolidation theory and three-dimensional finite element method. Numerical simulation is an essential method for researching the problems of foundation pit dewatering. This paper uses the finite element method to analyze the consolidation deformation of the foundation after groundwater extraction of a deep foundation pit excavation before the construction of the metro station.

2 Engineering background and geological conditions

Line 14 is an east-west subway line in the north of Xi'an city and an express line in the Xi'an subway network. The geological environment conditions along line 14 are relatively simple, with no geological disasters appearing, such as collapse, landslide, debris flow, ground collapse, or ground cracks. The depth of the groundwater level is about 10–20 m. The thickness of the submersible aquifer is about 50–80 m, and the annual variation of the groundwater level is about 1–3 m. The groundwater recharge mainly includes lateral runoff and atmospheric dewatering, and the discharge methods are runoff discharge, artificial extraction, and evaporation. The underground water level should be declined before the pit excavation to ensure the safety of metro station construction. However, groundwater dewatering will affect the groundwater level along the subway for a certain period and may cause local land subsidence and deformation (Roy and Robinson, 2009; Wang et al., 2012; Zeng et al., 2022).

2.1 Stratum characteristics

The landform along Metro Line 14 and the Cross section the Wei River terraces are shown in Figures 1, 2, respectively. The geomorphic units along Line 14 are as follows: the floodplain of the Wei River, the terrace of the Wei River, the floodplain of the Ba River, and the first and second terraces of the Ba River. The detailed characteristics of the strata along the Line 14 are described respectively from the surface as follows. Wei River's floodplain: mixed fill, Quaternary alluvial silty clay, Quaternary alluvial silt, and interbedded sand. The stratum of the first terraces of the Wei River are as follows: mixed fill soil, Quaternary alluvial loess-like soil, Quaternary alluvial soil, and fine sand. Ba River's floodplain: mixed fill soil, Quaternary alluvial loessial soil,

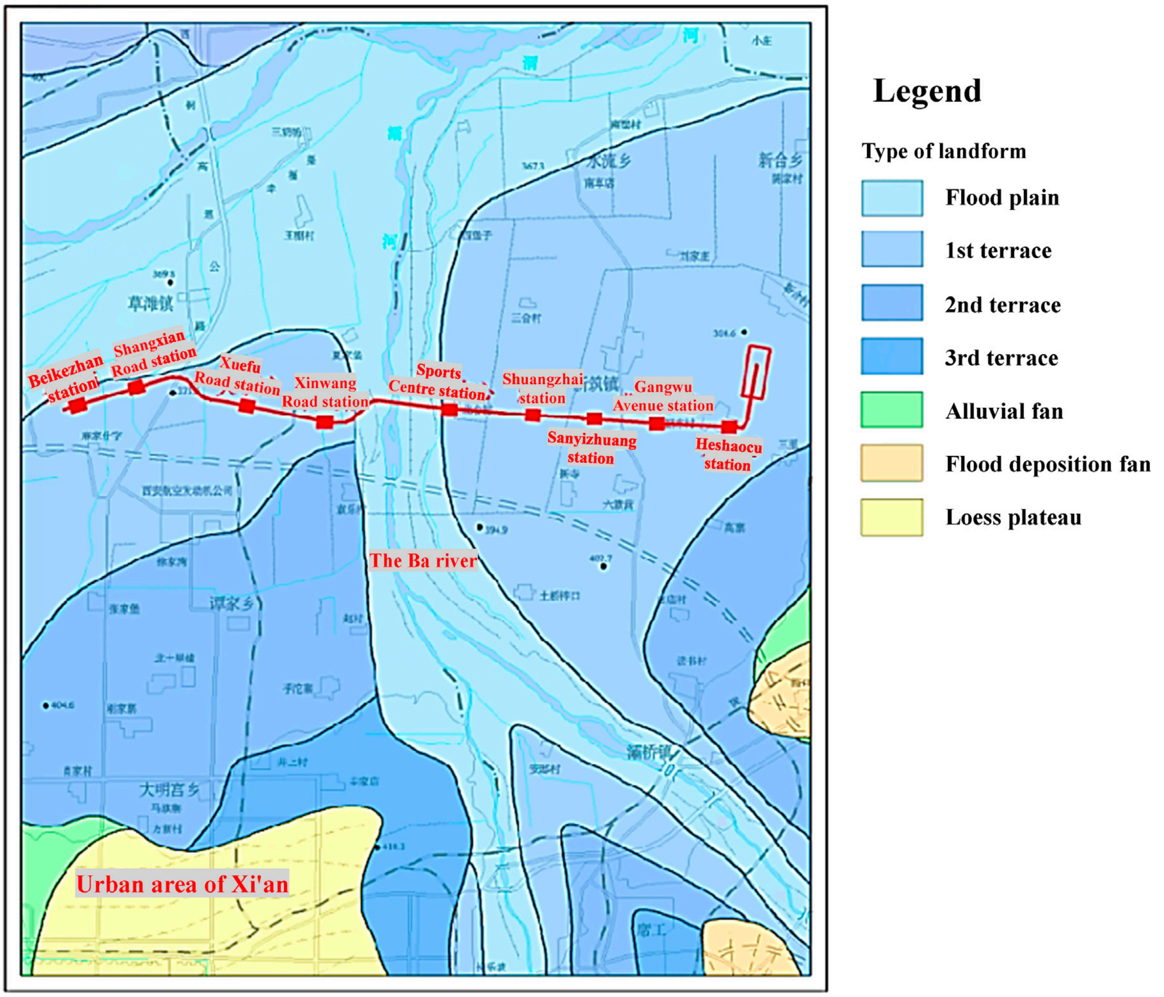

FIGURE 1
Topography along metro Line 14 of Xi'an.

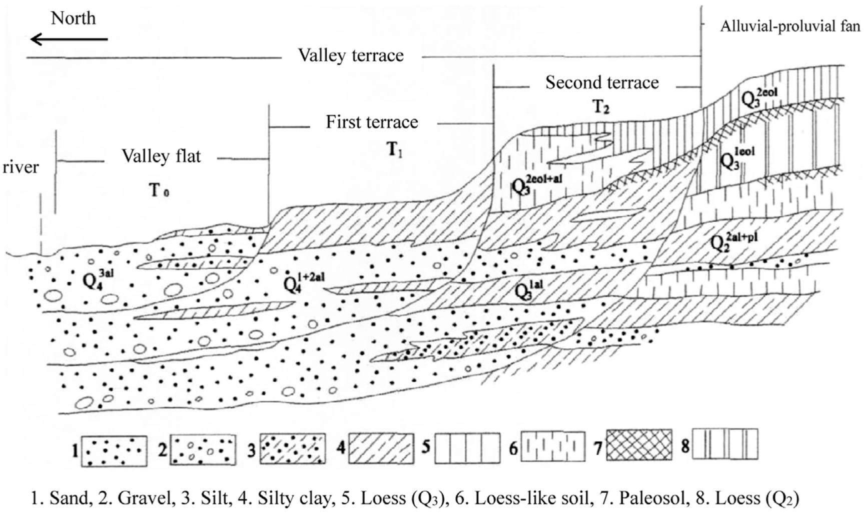

FIGURE 2
Cross section of Wei River terraces. 1. Sand, 2. Gravel, 3. Silt, 4. Silty clay, 5. Loess(Q3), 6. Loess-like soil, 7. Paleosol, 8. Loess(Q2).

TABLE 1 Summary table of underground water depth and permeability coefficient of metro stations on Line 14.

Station	Buried depth of groundwater (m)	Elevation of groundwater level (m)	Suggested value of permeability coefficient (m/d)
Shangxian Road station	12.00–13.50	358.06–359.06	25.0
Xuefu Road station	10.80–12.90	360.78–362.87	27.0
Xinwang Road station	13.60–14.30	361.96–362.78	22.0
Sports Centre station	11.70–13.30	363.30–364.60	27.0
Shuangzhai station	13.00–18.30	362.31–362.84	27.0
Sanyizhuang station	15.00–18.40	362.04–363.47	27.0
Gangwu Avenue station	19.10–21.00	361.23–361.81	23.0
Heshaocu station	22.00–25.50	359.34–361.34	25.0

Quaternary alluvial soil, and gravel. The first and second terraces of the Ba river: mixed fill soil, Quaternary alluvial loessial soil, Quaternary alluvial soil, and gravel.

2.2 Hydrogeological characteristics

The aquifers along metro Line 14 are mainly submersibles. The alluvial and diluvial strata are composed of sand and gravel, partially interspersed with clay interlayer. The groundwater depth along Line 14 is generally shallow, and the average permeability coefficient of the strata ranges from 15 to 60 m/d. The first terrace of Wei River: the buried depth of the groundwater level is 10.0–14.5 m. The primary aquifer is medium coarse gravel sand with strong water permeability. Ba River Valley and floodplain: the buried depth of the groundwater level is about 5.0–10.0 m, and the aquifer is the sand and gravel layer with high permeability. Wei River terrace: the groundwater depth is 12.5–26.0 m (gradually deepening from west to east). The primary aquifer is a medium coarse gravel layer with high permeability. The underground water depth and permeability coefficient of metro stations on Line 14 are listed in Table 1.

The atmospheric dewatering and irrigation infiltration mainly recharge the groundwater along Line 14, and the Ba River and groundwater are complementary in the wet season. The whole region of Line 14 is recharged by atmospheric dewatering, and the dynamic water level is consistent with the dewatering curve. The water level is shallow buried, and the infiltration volume is significant in rainy years or seasons. Generally, the lithologic grain size becomes finer with the increase of groundwater depth, and the permeability coefficient values will decrease. The lateral recharge of the Ba River will influence Line 14, which crosses the Ba River in the section between Xinwang Road and Sports Center.

TABLE 2 Estimation of water inflow of metro stations pit on Line 14.

Station	Geomorphic unit	Dewatering well	Drop of water level (m)	Prediction of water inflow (m^3/d)
Shangxian Road station	Valley flat of Wei river	55	6.0	6,500
Xuefu Road station	First terrace of Wei river	34	6.5	4,253
Xinwang Road station	First terrace of Wei river	35	5.5	3,170
Sports Centre station	First terrace of Ba river	20	13.0	3,537
Shuangzhai station	First terrace of Ba river	52	5.0	5,980

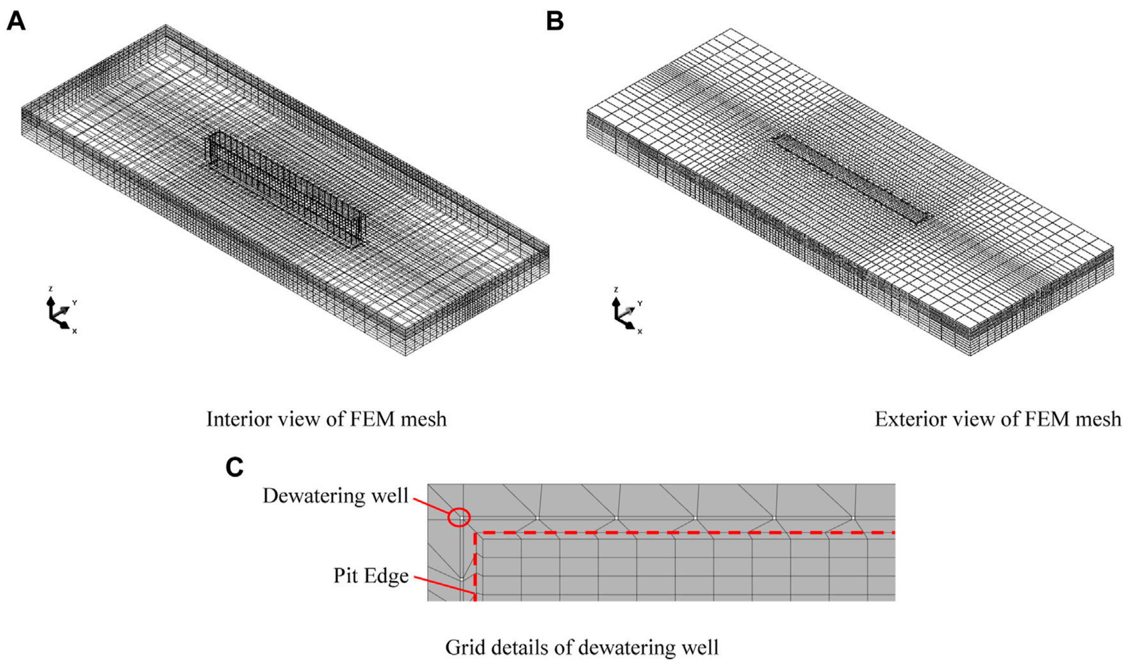

FIGURE 3
FEM model and meshing for typical subway station pit on Line 14. **(A)** Interior view of FEM mesh. **(B)** Exterior view of FEM mesh. **(C)** Grid details of dewatering well.

TABLE 3 Parameter value of soil for dewatering and consolidation analysis.

Soil layer	Density (g/cm^3)	Liquid limit w_L (%)	Void ratio e	η (g/ s·cm)	s (cm^{-1})	Modulus of compression E_s (MPa)	Cohesion C (kPa)	Friction angle φ (°)	Permeability coefficient k (cm/s)
Medium sand	1.85	10.8	0.606	1.01	3,000	10.8	0	32.5	3.34E-05
Silty clay	1.93	26.9	0.748	1.175	60,000	8.3	28	21.0	6.64E-08
Loess	1.90	22.7	0.709	1.088	40,000	8.1	29	20.0	1.63E-07

3 Hydraulic discharge prediction of metro line 14 dewatering

Xi'an metro Line 14 project has a total length of 14.4 km, and all station construction needs well dewatering. The hydraulic discharge of stations is estimated via the formula suggested in the standard of JGJ 120-2012. The stations of metro Line 14 are generally elongated, with a length of 164–527 m and a width of 19.7–24.7 m. The spacing of dewatering wells is generally 15–20 m, and the wells are arranged around the foundation pit. The water inflow of the foundation pit is close to a fixed value when the groundwater level is controlled to a certain depth via

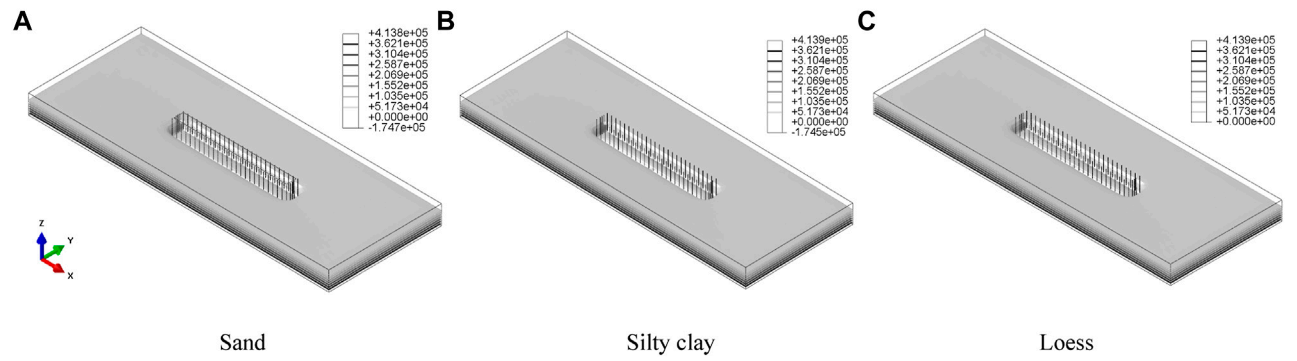

FIGURE 4
Isosurface contour of pore pressure after dewatering (Unit: Pa) **(A)** Sand **(B)** Silty clay **(C)** Loess.

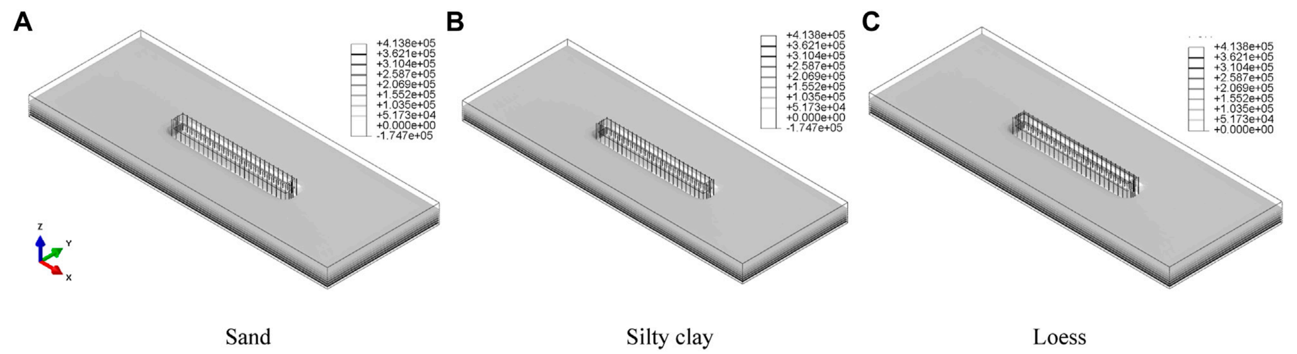

FIGURE 5
Isosurface contour of pore pressure after pit excavation (Unit: Pa) **(A)** Sand **(B)** Silty clay **(C)** Loess.

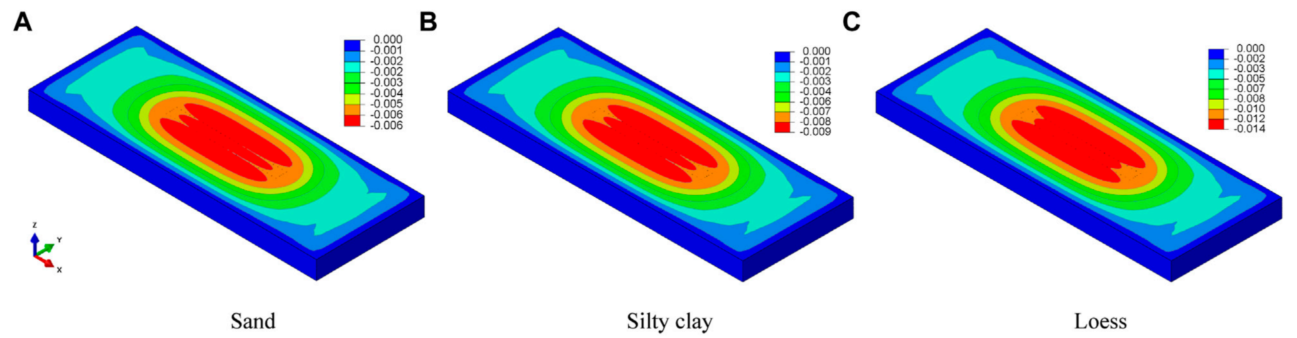

FIGURE 6
Settlement deformation contour after dewatering (Unit: m) **(A)** Sand **(B)** Silty clay **(C)** Loess.

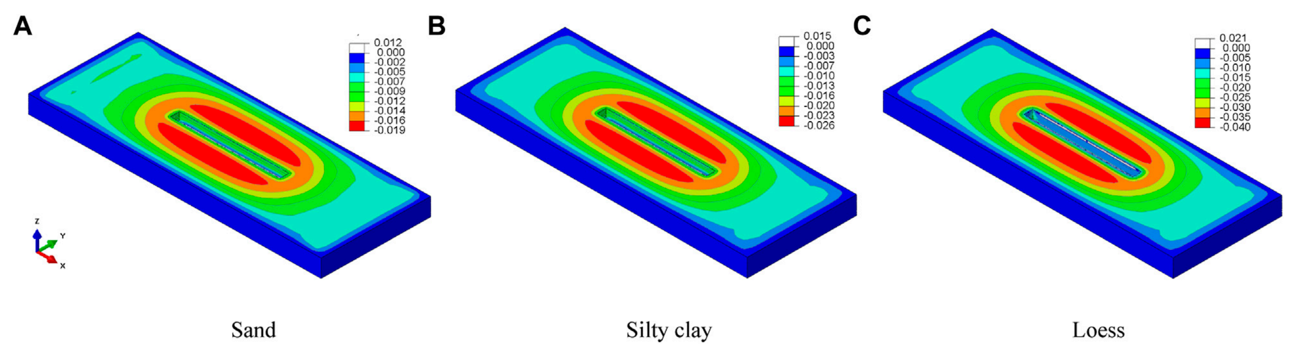

FIGURE 7
Settlement deformation contour after pit excavation (Unit: m). **(A)** Sand **(B)** Silty clay **(C)** Loess.

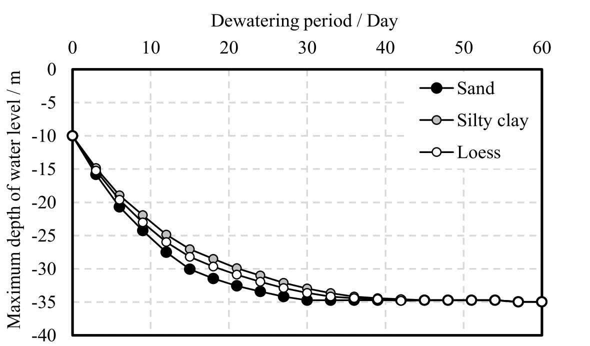

FIGURE 8
Relationship between maximum depth of groundwater level and dewatering period.

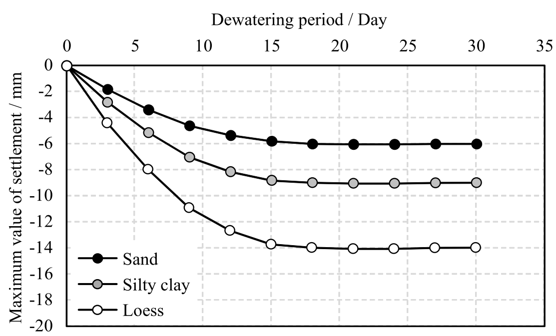

FIGURE 9
Relationship between maximum settlement and dewatering period.

foundation pit pumping, i.e., the pumped and the replenishment water reach a dynamic balance. The total water inflow of the metro station foundation pit is estimated using the calculation formula of the foundation pit water inflow of the non-integral well (see appendix E of the literature (Ministry of housing and urban-rural development of the People's Republic of China, 2012)). The group wells are simplified according to a whole large well for this formula. The calculation formula is as follows:

$$Q = \pi k \frac{H^2 - h^2}{\ln\left(1 + \frac{R}{r_0}\right) + \frac{h_m - l}{l}\ln\left(1 + 0.2\frac{h_m}{r_0}\right)} \tag{1}$$

Where Q is the total water inflow of foundation pit dewatering (m^3/d); k is the permeability coefficient of foundation (m/d); H is the submersible aquifer thickness (m); R is the influence radius (m); r_0 is the equivalent radius of foundation pit (m), $r_0 = \sqrt{A/\pi}$, where A is the pit area (m^2); h is the height of water level in the foundation pit after dewatering (m); l is the length (m) of the inlet water part of the filter, $h_m=(H+h)/2$. The water inflow estimation for the foundation pit of Line 14 station is shown in Table 2.

4 Numerical simulation of dewatering of metro station's pit

The Cartesian coordinate system is used to analyze this problem. The vertical direction is the z-axis, and the vertical direction is positive. The length, width, and depth of a typical metro station of Line 14 are 300 m, 25 m, and 20 m, respectively. The spacing and depth of the dewatering well are 20 m and 40 m, respectively. The horizontal distance between the well and the foundation pit boundary is 2 m, the thickness of the overlying layer on the metro station is 3 m, the rest is silty clay, and the depth of the groundwater level is 10 m. The model of the metro station foundation pit is divided into more than 60,000 eight-node hexahedral elements. The implicit consolidation calculation module of finite element software ABAQUS is used to analyze the problem of metro station pit dewatering (Simulia, 2017). The calculation model and element division of numerical simulation of foundation pit dewatering and station construction are shown in Figure 3.

In this paper, the permeability coefficient values for foundation soil are estimated by the modified Corson-Karman empirical formula (Singh and Wallender, 2008; Dang et al., 2015). The calculation formula is as follows:

TABLE 4 Summary of settlement deformation triggered by dewatering and pit excavation of metro station pit on Line 14.

Dewatering period (Day)	Groundwater level recovery period (Day)	Maximum settlement due to dewatering (mm)	Maximum settlement due to dewatering and pit excavation (mm)	Proportion of settlement due to dewatering
35	31	6/4 (Numerical analysis/Empirical formula)	19 (Numerical analysis)	31.6% (Numerical analysis)
49	48	9/5 (Numerical analysis/Empirical formula)	26 (Numerical analysis)	34.6% (Numerical analysis)
45	40	14/8 (Numerical analysis/ Empirical formula)	39 (Numerical analysis)	35.0% (Numerical analysis)

$$k = \frac{c_2 \rho_{wz} (e - e_0)^3}{s^2 \eta (1 + e - e_0)} \tag{2}$$

Where c_2 is the shape coefficient of soil particles (about .125), s is the specific surface area of soil particles, η is the viscosity coefficient of pore water, ρ_{wz} is the density of free pore water (about 1.0 g/cm^3), e is the pore ratio of the soil, e_0 is the ineffective pore ratio of the soil (depend on the liquid limit of the soil).

Three types of foundation soil (medium sand, silty clay, and loess) are used to analyze the influence of dewatering and consolidation deformation. The parameter value of soil for dewatering and consolidation analysis is shown in Table 3. The boundary conditions of the numerical model are set as follows: normal constraint boundary conditions are applied around the model, and three directions constraints are applied on the bottom surface of the model. A flow boundary is applied to the pumping well, and a zero pore pressure boundary is applied to the groundwater level (infiltration surface) (Wang et al., 2017; Wang et al., 2018; Zeng et al., 2021). The finite element method is used to calculate and analyze the dewatering and construction process of the typical station of Line 14. The numerical simulation predicts the time of groundwater level drop and the ground settlement (triggered by dewatering and pit excavation). The linear elastic constitutive model is used to calculate and analyze the concrete structure of the station. The density is 2.5 g/cm^3, the elastic modulus is 43 GPa, and the Poisson's ratio is .188.

5 Influence analysis of dewatering for loess metro station pit

The contour of pore water pressure and settlement deformation of the strata after dewatering and foundation pit excavation with sandy soil, silty clay, and loess stratum is shown in Figures 4–7. Where the pore water pressure of the stratum below the groundwater level before pit excavation is shown in the three-dimensional isosurface contour, the pore pressure unit is Pa, and the settlement unit is m.

The drop in water level mainly triggers the strata settlement due to the process of dewatering, and the settlement after station construction is mainly triggered by the pit excavation and supporting structure deformation. According to the theoretical calculation results, the settlement caused by the dewatering of each line project generally accounts for 10–40% of the total settlement. The finite element method is used to simulate the dewatering and construction of the typical metro station of Line 14. The analysis results show that the ground settlement is generally about 10–30 mm after the dewatering. The settlement value shows a trend of low in the west and high in the east along the metro line. The land subsidence of the metro station on the second terrace of the Ba River (loess stratum) due to dewatering is more significant than the first terrace of the Ba River (silty clay stratum). The flood plain and the first terrace of the Wei River (sandy soil stratum) have the lowest ground settlement after the dewatering. These results are mainly related to the soil properties of the stratum in this region. The loess stratum is prone to deformation after water loss due to the distribution of large pores. In contrast, the sand stratum will be compacted after dehydration, and the deformation of the stratum will be reduced. The finite element calculation results show that the silty clay stratum has the longest groundwater dewatering and recovery time, and the sandy soil stratum is the shortest. The relationships between the settlement deformation and underground water level of the typical metro station with sandy soil, silty clay, and loess stratum are shown in Figures 8, 9.

Based on the previous data, the finite element method is used to simulate the dewatering and construction of a typical station of Xi'an metro Line 14. According to the theoretical calculation results, the settlement caused by the dewatering before the metro station construction generally accounts for 10–40% of the total settlement. The predicted analysis shows that the ground settlement of Line 14 after the dewatering is generally about 10–30 mm. Most of the settlements for the metro construction are due to the deformation caused by underground excavation. A small part of the settlements is related to the influence of pipelines and basement deformation. According to the previous experience of the Xi'an metro, the settlement deformation due to the metro construction is within the controllable range. The formula suggested in the literature (Ministry of housing and urban-rural development of the People's Republic of China, 2012) is adopted to calculate the settlement deformation caused by foundation pit dewatering of a pumping well in a homogeneous aquifer (Xu et al., 2019; De Caro et al., 2020), and the estimation formula is as follows:

$$S = \psi_w \sum_{i=1}^{n} \frac{\Delta \sigma'_{zi} \Delta_{hi}}{E_{si}} \tag{3}$$

where s is the amount of formation deformation caused by dewatering (m), the empirical settlement coefficient ψ_w should be calculated according to local engineering experience, and it is better to obtain ψ_w=1 in general. $\Delta\sigma'_{zi}$ is the additional effective stress (kPa) at the middle point of the first layer of the ground caused by dewatering. For cohesive soil, the additional effective stress should be taken under the consolidation degree of soil at the end of dewatering. The thickness of Δh_i the ith layer soil (m); E_{si} is the compression modulus (kPa) of the ith layer soil, and n indicates the number of strata (In this paper, $n = 2$). Table 4 shows the summary results of ground settlement deformation caused by dewatering and construction of a typical station (loess strata) of metro Line 14, which is predicted by using the finite element method and empirical calculation formula. The ground settlement induced by pit dewatering also can be further analyzed via numerical methods taking the coupled thermo-hydro-mechanical influence into account (Liu et al., 2022a; Liu et al., 2022b; Zhang et al., 2022).

6 Conclusion

Based on the dewatering problem of the foundation pit of Xi'an Metro Line 14, the finite element method is used to analyze the influence of the foundation pit dewatering on land subsidence and ground deformation. The results show that the ground settlement induced by dewatering obtained by the numerical simulation are close to the results yield by the empirical formula suggested by the standard. The groundwater level in the sandy stratum has the fastest drops and recovers rate during dewatering compared with the clay (silty clay and loess) stratum. The sandy stratum's settlement indued by dewatering is relatively small, and the loess stratum has the most significant settlement induced by dewatering among the three kinds of strata. The proportion of settlement due to dewatering of the station construction in loess stratum is nearly 1/3 versus the total land subsidence.

Data availability statement

The original contributions presented in the study are included in the article/Supplementary Material, further inquiries can be directed to the corresponding author.

Author contributions

All authors listed have made a substantial, direct, and intellectual contribution to the work and approved it for publication.

Funding

The research described in this paper was funded by the National Natural Science Foundation of China (No. 51979225).

Conflict of interest

Author ZY was employed by China Railway First Survey and Design Institute Group Co., Ltd.

The remaining authors declare that the research was conducted in the absence of any commercial or financial relationships that could be construed as a potential conflict of interest.

Publisher's note

References

Attard, G., Winiarski, T., Rossier, Y., and Eisenlohr, L. (2016). Review: Impact of underground structures on the flow of urban groundwater. *Hydrogeology J.* 24 (1), 5–19. doi:10.1007/s10040-015-1317-3

Dang, F. N., Liu, H. W., Wang, X. W., Xue, H. B., and Ma, Z. Y. (2015). Empirical formulas of permeability of clay based on effective pore ratio. *Chin. J. Rock Mech. Eng.* 34 (9), 1909–1917. (In Chinese).

De Caro, M., Crosta, G. B., and Previati, A. (2020). Modelling the interference of underground structures with groundwater flow and remedial solutions in Milan. *Eng. Geol.* 2020 (105652), 105652. doi:10.1016/j.enggeo.2020.105652

Liu, N. F., Li, N., Li, G. F., Song, Z. P., and Wang, S. J. (2022). *Method for evaluating the equivalent thermal conductivity of a freezing rock mass containing systematic fractures*. Rock Mechanics and Rock Engineering. doi:10.1007/s00603-022-03038-9

Liu, N. F., Li, N., Wang, S. J., Li, G., and Song, Z. (2022). A fully coupled thermo-hydro-mechanical model for fractured rock masses in cold regions. *Cold Regions Sci. Technol.* 205 (2023), 103707. doi:10.1016/j.coldregions.2022.103707

Ministry of housing and urban-rural development of the People's Republic of China (2012). *Technical specification for retaining and protection of building foundation excavations*. JGJ 120-2012).

Pujades, E., De Simone, S., Carrera, J., Vazquez-Sune, E., and Jurado, A. (2017). Settlements around pumping wells: Analysis of influential factors and a simple calculation procedure. *J. Hydrology* 548, 225–236. doi:10.1016/j.jhydrol.2017.02.040

Pujades, E., Vazquez-Sune, E., Carrera, J., and Jurado, A. (2014). Dewatering of a deep excavation undertaken in a layered soil. *Eng. Geol.* 178, 15–27. doi:10.1016/j.enggeo.2014.06.007

Roy, D., and Robinson, K. E. (2009). Surface settlements at a soft soil site due to bedrock dewatering. *Eng. Geol.* 107 (3-4), 109–117. doi:10.1016/j.enggeo.2009.05.006

Shaqour, F. M., and Hasan, S. E. (2008). Groundwater control for construction purposes: A case study from Kuwait. *Environ. Geol.* 53 (8), 1603–1612. doi:10.1007/s00254-007-0768-9

Simulia, D. S. (2017). *Abaqus 6.17 help documentation*. Paris, France: Dassault Systems Corp.

Singh, P. N., and Wallender, W. W. (2008). Effects of adsorbed water layer in predicting saturated hydraulic conductivity for clays with Kozeny-Carman equation. *J. Geotechnical Geoenvironmental Eng.* 134 (6), 829–836. doi:10.1061/(asce)1090-0241(2008)134:6(829)

Sun, D., Zhao, Y. H., and Lu, Q. C. (2015). Vulnerability analysis of urban rail transit networks: A case study of shanghai, China. *Sustainability* 7 (6), 6919–6936. doi:10.3390/su7066919

Wang, J. X., Deng, Y., S., Wang, X. B., Liu, X. T., and Zhou, N. Q. (2022). Numerical evaluation of a 70-m deep hydropower station foundation pit dewatering. *Environ. Earth Sci.* 81 (14), 364–368. doi:10.1007/s12665-022-10493-8

Wang, J. X., Deng, Y. S., Ma, R. Q., Liu, X., Guo, Q., Liu, S., et al. (2018). Model test on partial expansion in stratified subsidence during foundation pit dewatering. *J. Hydrology* 557, 489–508. doi:10.1016/j.jhydrol.2017.12.046

Wang, J. X., Feng, B., Liu, Y., Wu, L., Zhu, Y., Zhang, X., et al. (2012). Controlling subsidence caused by dewatering in a deep foundation pit. *Bull. Eng. Geol. Environ.* 71 (3), 545–555. doi:10.1007/s10064-012-0420-0

Wang, J. X., Feng, B., Yu, H. P., Guo, T., Yang, G., and Tang, J. (2013). Numerical study of dewatering in a large deep foundation pit. *Environ. Earth Sci.* 69 (3), 863–872. doi:10.1007/s12665-012-1972-9

Wang, J. X., Liu, X. T., Wu, Y. B., Liu, S., Wu, L., Lou, R., et al. (2017). Field experiment and numerical simulation of coupling non-Darcy flow caused by curtain and pumping well in foundation pit dewatering. *J. Hydrology* 549, 277–293. doi:10.1016/j.jhydrol.2017.03.070

Xu, Y. S., Yan, X. X., Shen, S. L., and Zhou, A. N. (2019). Experimental investigation on the blocking of groundwater seepage from a waterproof curtain during pumped dewatering in an excavation. *Hydrogeology J.* 27 (7), 2659–2672. doi:10.1007/s10040-019-01992-3

Zeng, C. F., Liao, H., Xue, X. L., Long, S. C., Luo, G. J., Diao, Y., et al. (2022). Responses of groundwater and soil to dewatering considering the barrier effect of adjacent metro station on multi-aquifers. *J. Hydrology* 612, 128117. doi:10.1016/j.jhydrol.2022.128117

Zeng, C. F., Song, W. W., Xue, X. L., Li, M. K., Bai, N., and Mei, G. X. (2021). Construction dewatering in a metro station incorporating buttress retaining wall to limit ground settlement: Insights from experimental modelling. *Tunn. Undergr. Space Technol.* 116, 104124. doi:10.1016/j.tust.2021.104124

Zhang, Y. W., Fan, S. Y., Yang, D. H., and Zhou, F. (2022). Investigation about variation law of frost heave force of seasonal cold region tunnels: A case study. *Front. Earth Sci.* 9, 806843. doi:10.3389/feart.2021.806843

Zhou, N. Q., Vermeer, P. A., Lou, R. X., Tang, Y., and Jiang, S. (2010). Numerical simulation of deep foundation pit dewatering and optimization of controlling land subsidence. *Eng. Geol.* 114 (3-4), 251–260. doi:10.1016/j.enggeo.2010.05.002